Determination of a Diagnostic Signature for World Trade Center Dust using Scanning Electron Microscopy Point Counting Techniques

By Gregory P. Meeker, Amy M. Bern*, Heather A. Lowers, and Isabelle K. Brownfield

Open-File Report 2005 - 1031

U.S. Department of the Interior
U.S. Geological Survey, Denver Federal Center, Denver, CO 80225

*Current address: U.S. Environmental Protection Agency, National Enforcement Investigations Center, Denver Federal Center, Denver, CO 80225

Introduction

The tragedy of the September 11, 2001, collapse of the World Trade Center (WTC) towers and other buildings in and adjacent to the WTC site produced a dust cloud that was visible from space and covered much of lower Manhattan in millimeters to centimeters of extremely fine powdered material. This material was inhaled and ingested by thousands of people on the day of the event and for several days afterward. In addition, thousands of apartments, offices, and public buildings were contaminated by the dust through a variety of pathways. The short-term medical effects of this exposure were manifested in what became known as the World Trade Center (WTC) cough, documented as respiratory and other health problems among many of those who were exposed (Gavett and others, 2003; Prezant and others, 2002). Potential long-term medical effects of this event may not be known for many years. Several studies have examined various components of the dusts generated by the collapse of the WTC (Meeker and others, 2005; Plumlee and others, 2005; Badger and others, 2004; Yiin and others, 2004; McGee, 2003; Offenberg and others, 2003; Chatfield and Kominsky, 2002; Lioy and others, 2002, Millette and others, 2002; Clark and others, 2001).

Concerns remain about the possible presence of WTC dust in indoor and outdoor environments in Lower Manhattan and surrounding areas. Identification of contamination from WTC dust more than 3 years after the event is complicated by dilution and possible variations in relative abundance of dust components arising from factors such as exposure to moisture, distance from the WTC site, and elevation. Detection of contaminants of potential concern (COPC) including asbestos, crystalline silica, lead, and man-made vitreous fibers (MMVF) originating from WTC dust is complicated by possible contributions of these materials from a variety of other unrelated sources including construction materials, asbestos-containing insulation, and lead-based paint.

Identification of WTC contamination would be easier if unique components or ratios of components were present in WTC dust that could be identified by routine analytical techniques. This preliminary report seeks to quantitatively define the fine-particle fraction of WTC dust for the purpose of identifying a diagnostic signature. The signature could then be used by those working on this and other aspects of the WTC dust contamination issue in order to identify low levels of residual WTC dust. The analytical procedures in this report are not intended to be used as routine methods for analysis of samples; they were developed to obtain an accurate quantitative determination of the relative abundances of components in bulk WTC dust. It is anticipated that a final report will follow after background samples are collected and analyzed for possible WTC dust signature components.

Sample Preparation

Samples were collected from outdoor and indoor locations at various distances from the WTC site. Samples USGS 4, 6, and 12 were collected from ground level between September 16 – 17, 2001, at distances of 0.80, 0.60, and 0.55 km, respectively, from the

center of the WTC site. These samples were wetted by one rain storm prior to collection. Sample USGS 36, collected on September 12, 2001, was obtained inside an apartment on the 30th floor of a building 2 blocks (0.40 km) from the WTC site. Details of sample collection procedures and locations for the above samples are given in Clark and others (2001) and Swayze and others (2005). Sample LM2 is an outdoor sample collected on September 16 – 17, 2001, approximately 0.70 km east of the WTC site. Sample L18-2 was collected indoors on November 19, 2001, from an area adjacent to the WTC site (0.25 km west). For further details on samples LM2 and L18-2 see Lioy and others (2002).

Sample preparation methods follow a modified version of the approach outlined in Bern and others (2005). Representative aliquots of WTC bulk dust samples were dry sieved through a 150 μm (100 mesh) ultrasonic sieve. A 0.2 g aliquot of the sieved sample was suspended in 125 mL of isopropanol alcohol. Using an Eppendorf pipette with 1 mm diameter tip opening, six 20 μL drops of the suspension were added to a Millipore filter apparatus with several milliters of alcohol in the funnel and a carbon coated 25 mm cellulose filter having a 0.4 μm pore size. The amount of sample was adjusted to yield coverage of approximately 2 – 4 percent on the filter. Coverage greater than about 10 percent causes particles to overlap, which can cause analytical errors. The filter was placed on a scanning electron microscope (SEM) stub using carbon adhesive tab. After drying, the stub was carbon coated using a carbon evaporator prior to analysis in the SEM.

The above method worked well for all components except MMVF. For some sample preparations, the abundance of MMVF particles was significantly reduced on the analytical filters relative to their abundance in bulk dust as observed by optical microscopy. The reason for fiber loss is unknown but may result from charging of the glass fibers by the electron beam during analysis in the SEM. To more accurately determine MMVF abundances, new aliquots of the samples were prepared by pipetting the suspension directly onto conductive carbon tape and analyzed in the SEM as described below.

Analytical Methods

Analyses were performed using a JEOL 5800LV electron microscope equipped with an Oxford ISIS energy dispersive x-ray spectrometer (EDS) and analysis system. Typical analytical conditions were 15 KeV accelerating voltage, 0.5-5 nA beam current, and zero-degree tilt. Data were processed using standardless quantitative analysis and compared to values obtained for BIR-1G glass (Meeker and others, 1998). Precision and accuracy vary for each element. Elemental values depend on particle size and shape but generally did not exceed 10 percent relative error for accuracy and 5 percent relative error for precision for Si, Al, Mg, Ca, and Fe, and 20 percent relative error for accuracy and 10 percent relative error for precision for Na, K, Ti, and Mn (Bern and others, 2005; Meeker and others, 2003).

For the filter samples, area-percentage coverage of total sample was determined using binary representations of backscattered electron images. Area fraction of individual particles was determined by direct measurement using digital images. The chemistry of each particle equal to or larger than 3 μm in the 500X magnification field of view (FOV) was determined and binned according to particle type. This process was also performed at 2,000 times magnification for all particles less than 3 μm. Twenty randomly selected fields of view at each magnification were analyzed for each sample. The number of particles counted on each sample ranged from 900 to over 3,000 depending on the density of filter coverage. The results for each magnification were normalized to equal area and combined to quantify particle abundances.

Particles were binned by type based on extensive analysis of WTC dust by multiple analytical techniques (Meeker and others, 2005, and references therein). Typical particle fields are shown in Figure 1. Particle types used in this study are listed in Table 1.

The area percentage of MMVF was determined separately for each sample by analyzing one field at 100 times magnification on a separate aliquot of sample prepared as described above. In addition, five fields on two samples (WTC 4 and WTC 6) were analyzed for all particles. These results were compared to the results obtained by the filter method. Particle size (length x width) distributions for the major components in each sample (< 150 μm size fraction) were also determined.

Results

Component analysis for the six WTC bulk samples is summarized in Table 1 and Figures 2 - 7. All of the samples show three primary components – gypsum, phases compatible with concrete, and MMVF. The additional particle types shown in Table 1 were found in most samples. The data demonstrate that the most consistent particle-type abundance ratios occur within the MMVF, i.e., slag wool, rock wool, and soda-lime glass. In all samples, slag wool is the dominant MMVF component while rock wool and soda-lime glass fibers occur in all samples at similar relative abundances below approximately 10 to less than 1 percent total MMVF (Table 1). One exception to this observation was identified in a single field counted at 100 times magnification on sample L18-2. In this field, a single large soda-lime glass fiber and a single large rock wool fiber were found; these two fibers significantly affected MMVF relative particle abundances. If these two fibers are not included, the relative MMVF abundances for this sample are similar to those for the other samples. A second field on this sample was counted at 100 times magnification; the resulting data were consistent with the other samples (Table 2). In all samples, the relative abundances of rock wool and soda-lime glass fibers are based on a small number of fibers; thus, the statistical significance of reported proportions of these fiber types is correspondingly low.

Table 1. Range in area percent of major and minor components for all samples.

Particle Type	Comment	Percent Range, Outdoor	Percent Range, Indoor
Gypsum	Includes all Ca sulfate particles	26.3 – 53.3	63.3 – 63.7
Concrete	All phases compatible with hydrated cement	19.3 – 30.8	14.0 – 21.0
MMVF* Total		20.3 – 40.6	9.5 – 19.2
Slag wool	Based on table 2, field 2	91.7 – 98.1	89.5 – 93.3
Rock wool	Based on table 2, field 2	0 – 6.6	5.2 – 5.8
Soda-lime glass	Based on table 2, field 2	0 – 6.0	0.9 – 5.3
Chrysotile	Bundles and single fibers	0.4 – 1.8	0 – 0.1
Silica	Primarily crystalline	0.8 – 3.4	0.4 – 0.7
Ti-rich	Primarily Ti and Ti oxide	0 – 0.1	0 – 0.6
Zn-rich	Primarily Zn and Zn oxide	0.2 – 0.4	0.1 – 0.6
Pb-rich	Primarily Pb and Pb oxide	N.D.	0 – 0.03
Fe-rich	Primarily Fe and Fe oxide	0.2 – 1.3	0.1 – 1.1
Other	Identified but not binned	2.6 – 5.9	1.4 – 2.6
Unidentified	Could not be classified based on bulk chemistry	0.2 – 1.4	0 – 0.1

*Man-made vitreous fibers (MMVF)

All samples also contain gypsum and concrete phases. In the outdoor samples, these components, along with total MMVF, vary in relative abundance. This variation is likely related to samples having been exposed to moisture and precipitation, which caused varying amounts of gypsum dissolution prior to sample collection. The two indoor samples, unaffected by precipitation, have much less variable compositions.

By far, the most abundant nonfibrous particles in all samples are gypsum and concrete. Particle size distributions for these components (Figs. 8 and 9) suggest relationships to distance and elevation. Percent frequency is compared to area and maximum diameter, as measured on the SEM. The majority of these nonfibrous particles in each sample have similar particle area distributions with the majority of particles in the range from 0.3 to 3 μm^2. Sample L18-2, collected adjacent to the WTC site, is characterized by a somewhat higher concentration of particles in the 3 to 300 μm^2 size range. Particles in samples USGS 4 and 6 fall at slightly higher values of total area, between 1 and 300 μm^2, than in the other outdoor samples. The effect of particle-size distribution as a function of distance is most clearly seen in Figure 9 where samples L18-2 and USGS 36 clearly deviate from the other samples with respect to size distribution. Sample L18-2, the closest sample to the WTC site, shows a higher abundance of larger diameter particles. Sample USGS 36, collected on the 30th floor of a building, shows a higher abundance of smaller diameter particles. MMVF diameters for all samples combined are given in Table 3. The distributions of MMVF diameters display no clear relationship to distance from the WTC site.

Table 2. Results from sample L18-2

Component	Comment	Area Percentage
Slag wool	Field 1, all fibers counted	52.1
Rock wool	Field 1, all fibers counted	9.6
Soda-lime glass	Field 1, all fibers counted	38.3
Slag wool	Field 1, two large fibers removed	86.5
Rock wool	Field 1, two large fibers removed	2.9
Soda-lime glass	Field 1, two large fibers removed	10.7
Slag wool	Field 2, all fibers counted	89.5
Rock wool	Field 2, all fibers counted	5.2
Soda-lime glass	Field 2, all fibers counted	5.3

Table 3. Diameter data for man-made vitreous fibers
All Samples Combined

	Rock wool	Slag wool	Soda-lime glass
Minimum	0.2	0.1	0.1
Maximum	15.6	21.0	13.0
Average	3.8	4.7	4.0

Conclusions

Six bulk WTC dust samples, collected from locations in different directions, elevations, and from outdoor and indoor environments show relatively consistent abundance ratios of major and minor components. For the purposes of identification of WTC dust, these abundance ratios appear to be within the necessary limits of variability. Furthermore, the critical dust components can be identified easily and quickly using routine SEM and x-ray microanalysis techniques.

Data presented here suggest that the presence and relative abundance of the three MMVF components – slag wool, rock wool, and soda-lime glass – along with the presence of concrete particles and gypsum could be used as a primary diagnostic signature for WTC dust. Secondary signature components could include FeO_x, ZnO_x, silica, and chrysotile.

An analysis strategy for routine samples could evolve using rapid scans of settled dust by SEM to look for the presence of MMVF. If found, these fibers could then be analyzed using EDS to determine fiber compositions. If the majority of fibers (> 85 percent) detected were of slag wool composition, or if slag wool was found at a predetermined critical concentration, the sample would then be searched for gypsum and concrete particles along with the other two MMVF components. Further confirmation of the presence of WTC dust could then be reached by looking for secondary components in the approximate abundances found in this study. Alternatively, if slag wool, gypsum, and concrete were present, the sample could then be analyzed for contaminants of potential concern such as asbestos, lead, and potentially problematic organic compounds.

Because the dust component ratios are shown here to be relatively constant from sample to sample, it should be possible for health workers to establish conservative health-based criteria for COPC relative to the abundance of slag wool. If slag wool fibers are not found in settled dust samples above a predetermined critical level, it is unlikely that COPC derived from the WTC could be present at significant levels in the samples.

A successful application of these data to the WTC dust contamination problem in specific environments will depend on the degree to which WTC dust components are found in typical background samples. For example, MMVF are a major component of some acoustical ceiling tiles. Indoor environments with these tiles would be more likely to contain MMVF in settled dust than environments with other ceiling materials. Recently remodeled buildings are more likely to contain settled dust with gypsum and even concrete. In difficult cases, the size distribution data presented here might prove useful in distinguishing WTC source materials from similar materials from other sources. Dilution effects and any variations that might occur at greater distances from the WTC site must also be considered.

Acknowledgements

The authors wish to thank Dr. Paul Lioy for providing two of the samples used in this study. This report has been greatly improved by reviews and discussions with Ed du Bray and Todd Hoefen. This work was funded by the U.S. Geological Survey.

Literature Cited

Badger, S.R., Rickabaugh, K.P., Potter, M.S., Scheetz, B.E., Bhattacharjee, H.R., and Lee, R.J., 2004, World Trade Center particulate contamination signature based on dust composition and morphology: Microscopy and Microanalysis, v. 10, suppl. 2, p. 948 - 949CD.

Bern, A.M. Brownfield, I.K., and Meeker, G.P., 2005, Preparation and analysis of soil samples for measurement of asbestos content by scanning electron microscopy and energy dispersive spectrometry: U.S. Geological Survey Open-File Report, in preparation.

Chatfield, E.J. and Kominsky, J.R., 2002, Characterization of particulate found in apartments after destruction of the World Trade Center; Chatfield Technical Consulting Limited, Mississauga, Ontario, Canada.

Clark, R.N., Green, R.O., Swayze, G.A., Meeker, G.P., Sutley, S., Hoefen, T.M., Livo, K. E., Plumlee, G., Pavri, B., Sarture, C., Wilson, S., Hageman, P., Lamothe, P., Vance, J. S., Boardman, J., Brownfield, I., Gent, C., Morath, L. C., Taggart, J., Theodorakos, P. M., and Adams, M. 2001, U.S. Geological Survey Open File Report 01-0429.

Gavett, S.H., Haykal-Coates, N., Highfill, J.W., Ledbetter, A.D., Chen, L.C., Cohen, M.D., Harkema, J.R., Wagner, J.G., and Costa, D.L., 2003, World Trade Center fine particulate matter causes respiratory tract hyperresponsiveness in mice: Environmental Health Perspectives, v. 111, no. 7, p. 981 - 991.

Lioy, P.J., Weisel, C.P., Millette, J.R., Eisenreich, S., Vallero, D., Offenberg, J., Buckely, B., Turpin, B., Zhong, M., Cohen, M.D., Prophete, C., Yang, I., Stile, R., Chee, G., Johnson, W., Porcja, R., Alimokhtari, S., Hale, R.C., Weschler, C., and Chen, L.C., 2002, Characterization of the dust/smoke aerosol that settled east of the World Trade Center (WTC) in lower Manhattan after the collapse of the WTC 11 Septemeber 2001: Environmental Health Perspectives, v. 110, no. 7, p. 703 - 714.

McGee, J.K. and others, 2003, Chemical analysis of World Trade Center fine particulate matter for use in toxicologic assessment: Environmental Health Perspectives, v. 111, no. 7, p. 972 - 980.

Meeker, G.P., Taggert, J.E, and Wilson, S.A., 1998, A basalt glass standard for multiple microanalytical techniques: Microscopy and Microanalysis, v. 4, suppl. 2, p. 240 - 241.

Meeker, G.P., Bern, A.B., Brownfield, I.K., Lowers, H.A., Sutley, S.J., Hoefen, T.M., and Vance, J.S., 2003, The composition and morphology of amphiboles from the Rainy Creek complex, near Libby, Montana: American Mineralogist, 88, p. 1955 - 1969.

Meeker and others, 2005, Materials characterization of dusts generated by the collapse of the World Trade Center, *in* Urban Aerosols and Their Impacts: Lessons Learned from the World Trade Center Tragedy, American Chemical Society, in press.

Millette, J.R., Boltin, R., Few, P., and Turner, W. Jr., 2002, Microscopical studies of World Trade Center disaster dust particles: Microscope, v. 50, no. 1, p. 29 - 35.

Offenberg, J.H., Eisenreich, S.J., Chen, L.C., Cohen, M.D., Chee, G., Prophete, C., Weisel, C., and Lioy, P.J., 2003, Persistent organic pollutants in the dusts that settled across lower Manhattan after September 11, 2001: Environmental Science and Technology, v. 37, p. 502 - 508.

Plumlee and others, 2005, Inorganic chemical composition and chemical reactivity of settled dust generated by the World Trade Center building collapse, *in* Urban Aerosols and Their Impacts: Lessons Learned from the World Trade Center Tragedy, American Chemical Society, in press.

Prezant, D.J., Weiden, M., Banauch, G.I., McGuinness, G., Rom, W.N., Aldrich, T.K., and Kelly, K.J., 2002, Cough and bronchial responsiveness in firefighters at the World Trade Center site: The New England Journal of Medicine, v. 347, no. 11, p. 806 - 842.

Swayze and others, 2005, Spectroscopic and x-ray diffraction analyses of asbestos in the World Trade Center dust, *in* Urban Aerosols and Their Impacts: Lessons Learned from the World Trade Center Tragedy, American Chemical Society, in press.

Yiin, L., Millette, J.R., Vette, A., Ilacqua, V., Quan, C., Gorczynski, J., Kendall, M., Chen, L.C., Weisel, C.P., Buckley, B., Yang, I., Lioy, P.J., 2004, Comparisons of the dust/smoke particulate that settled inside the surrounding buildings and outside on the streets of southern New York City after the collapse of the World Trade Center, September 11, 2001: Journal of the Air and Waste Management Association, v. 54, p. 515 – 528.

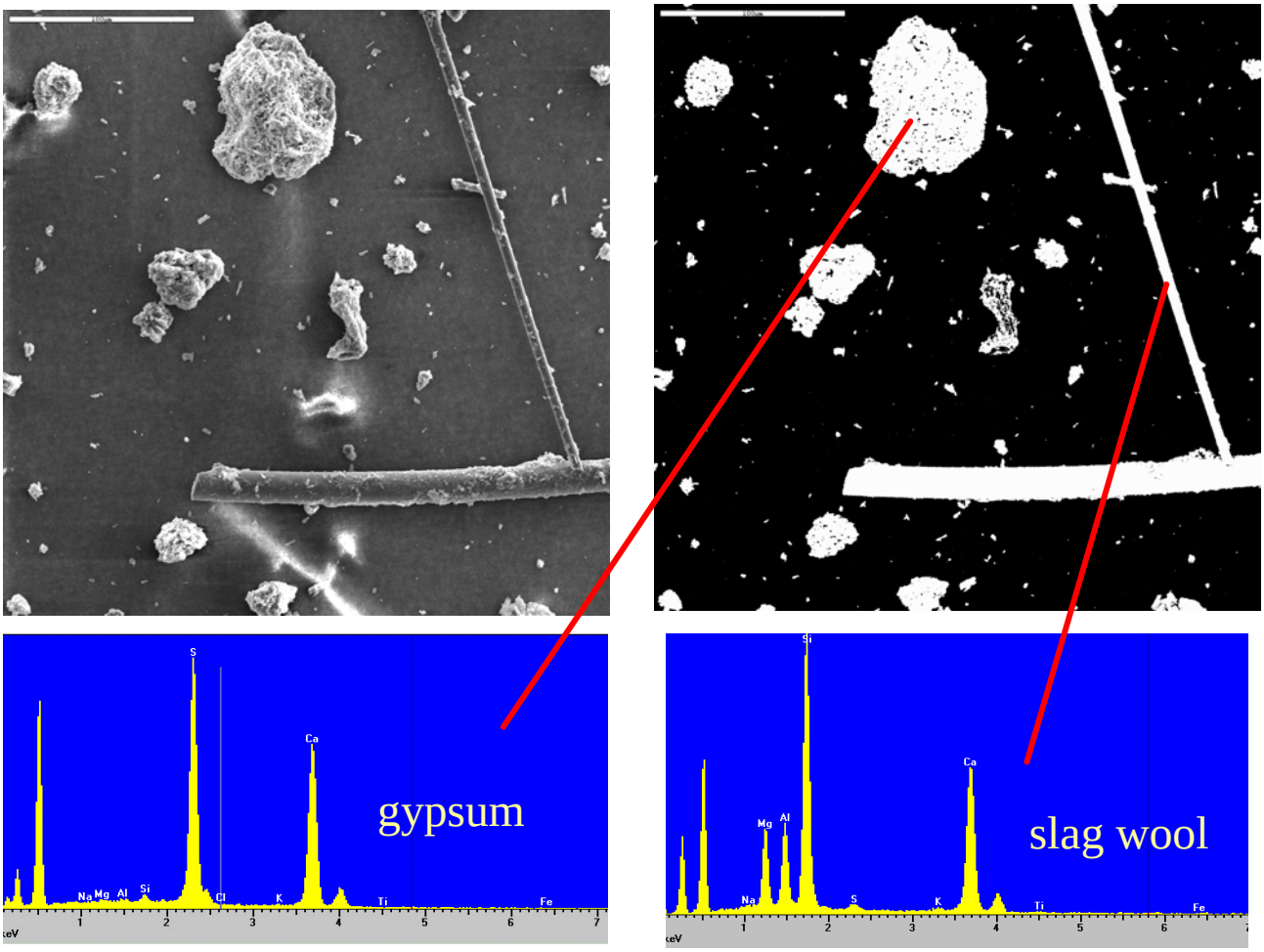

Figure 1. Secondary electron image of a typical field at 500 times magnification (left). The same image shown in binary backscatter mode is on the right. EDS spectra are shown for gypsum and slag wool.

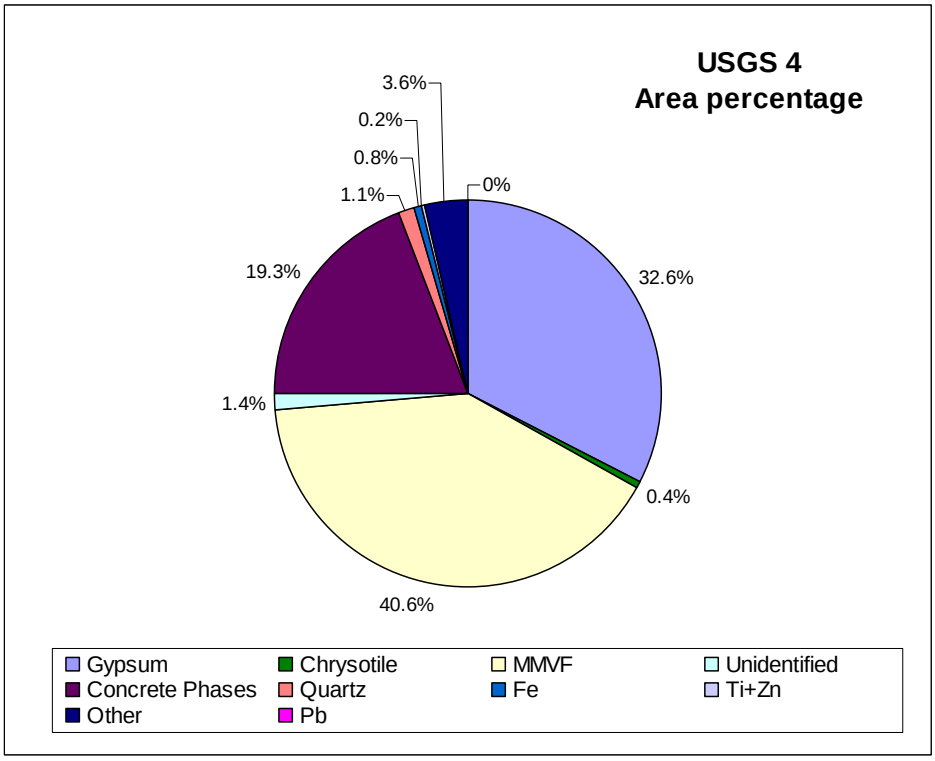

Figure 2. Relative abundances of dust components for outdoor sample USGS 4, collected 0.80 km south of the World Trade Center site. Components are shown in clockwise order as listed below each pie chart. Percentage of each component is given.

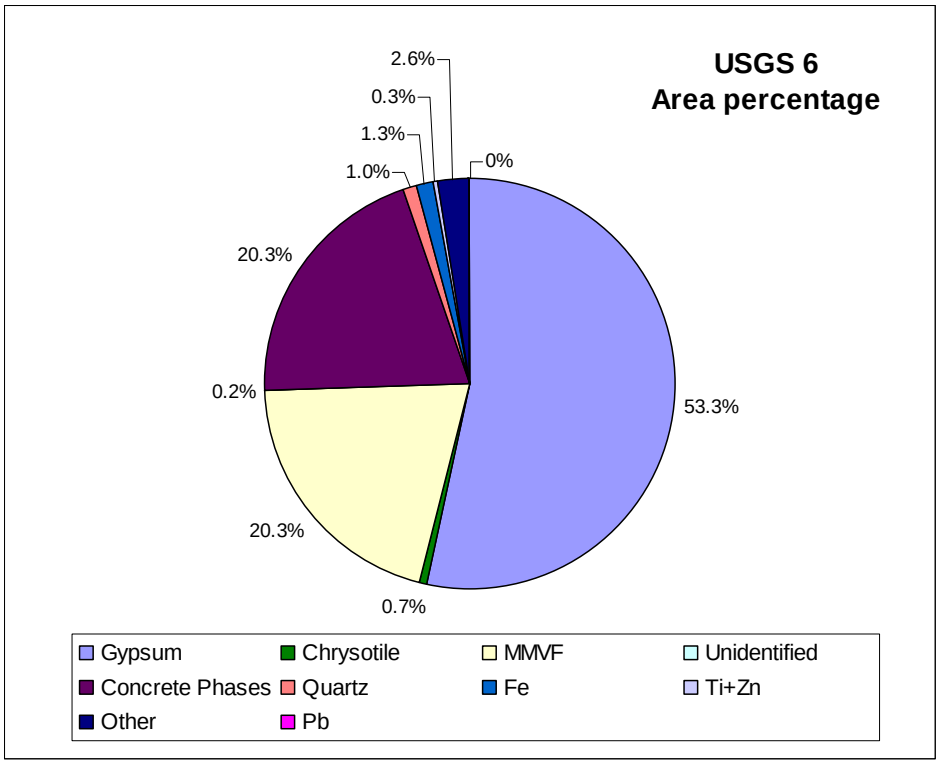

Figure 3. Relative abundances of dust components for outdoor sample USGS 6, collected 0.60 km south of the World Trade Center site. Components are shown in clockwise order as listed below each pie chart. Percentage of each component is given.

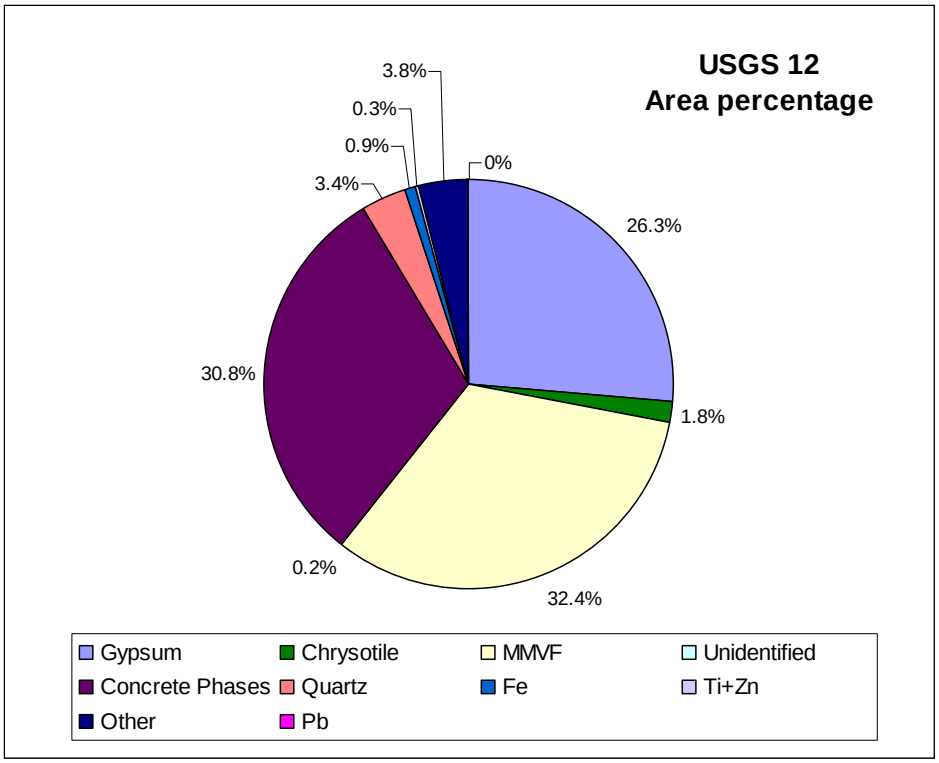

Figure 4. Relative abundances of dust components for outdoor sample USGS 12, collected 0.55 km south of the World Trade Center site. Components are shown in clockwise order as listed below each pie chart. Percentage of each component is given.

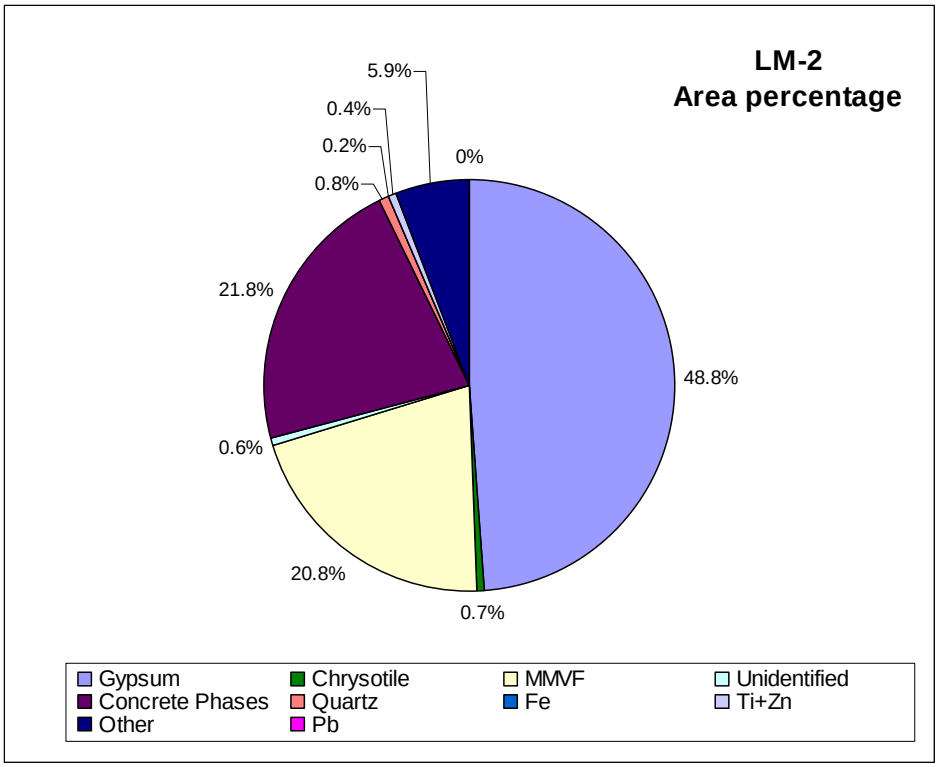

Figure 5. Relative abundances of dust components for outdoor sample LM-2, collected 0.70 km south of the World Trade Center site. Components are shown in clockwise order as listed below each pie chart. Percentage of each component is given.

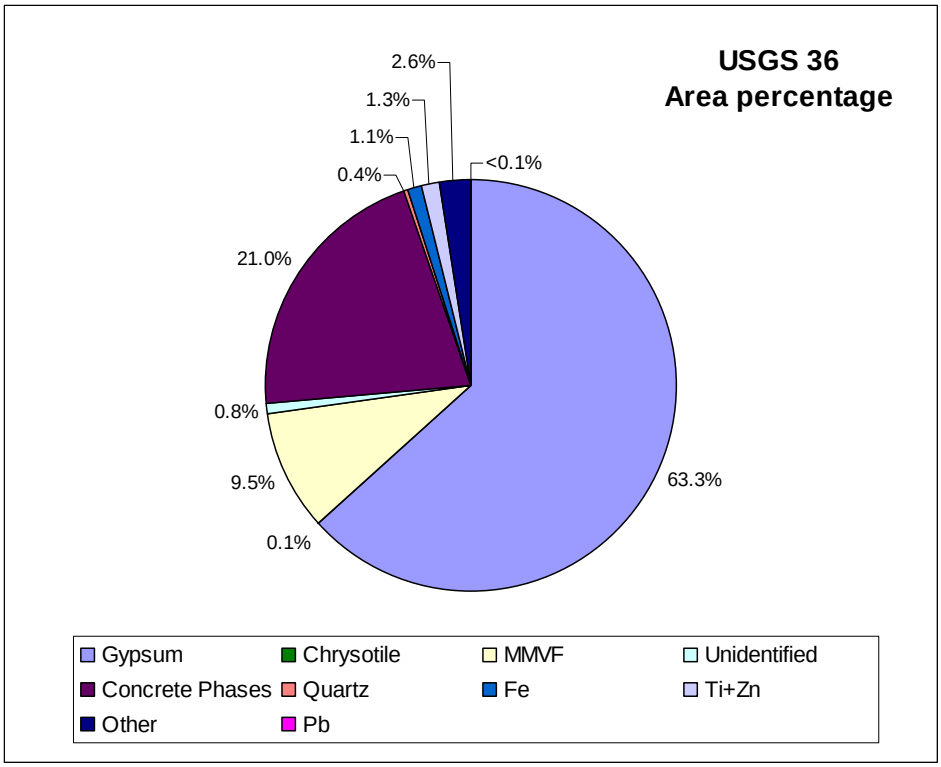

Figure 6. Relative abundances of dust components for indoor sample USGS 36, collected from a 30th floor apartment, 0.40 km south of the World Trade Center site. Components are shown in clockwise order as listed below each pie chart. Percentage of each component is given.

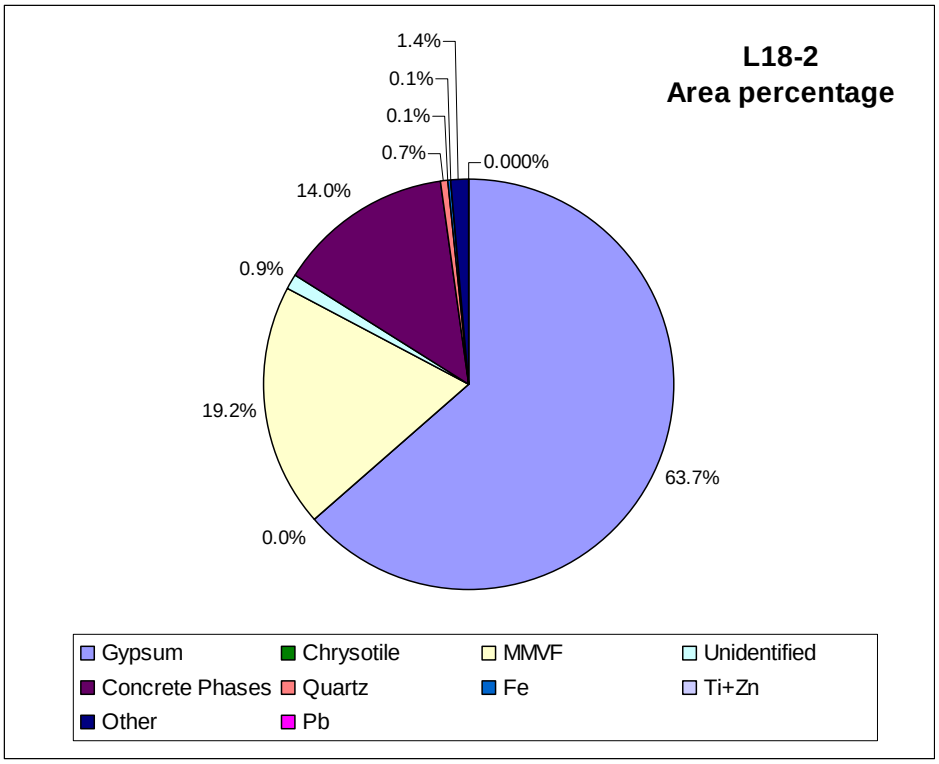

Figure 7. Relative abundances of dust components for indoor sample L18-2, collected on the west side of the World Trade Center site. Components are shown in clockwise order as listed below each pie chart. Percentage of each component is given.

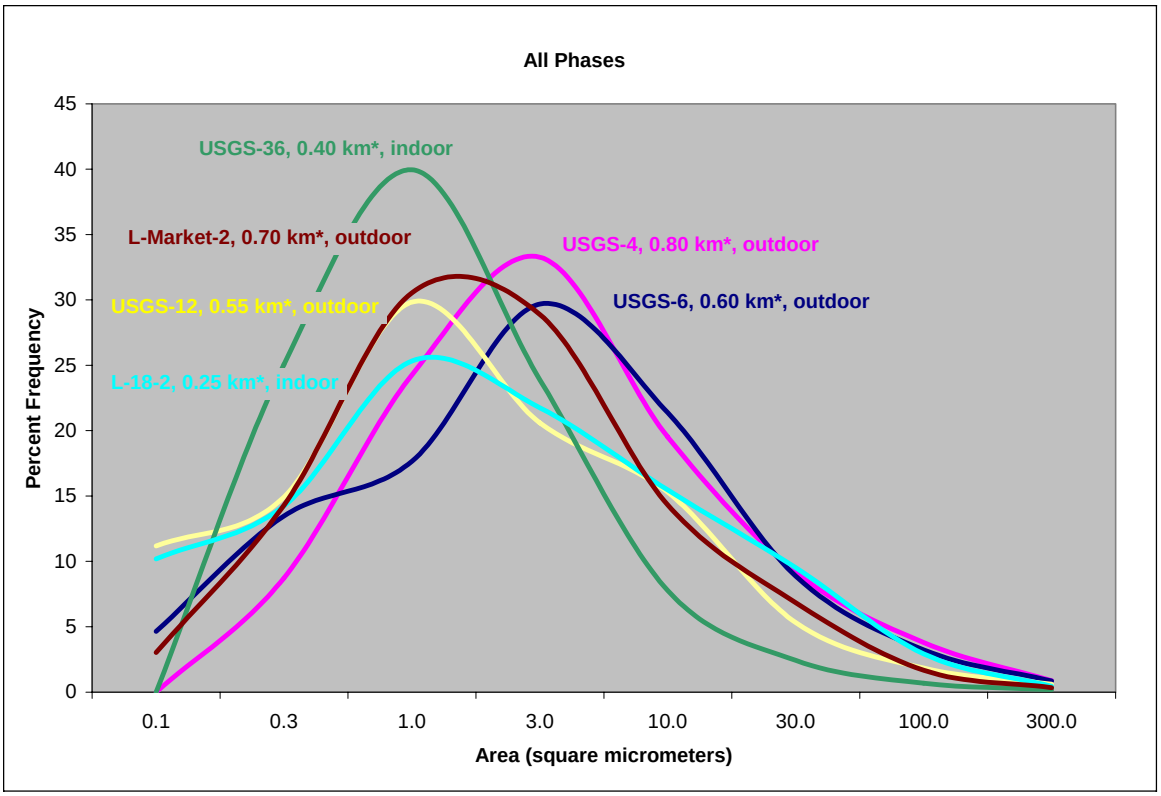

Figure 8. Particle size data for each sample presented as area (length x average width) vs. percentage frequency. *All distances are approximate kilometers from the center of WTC plaza.

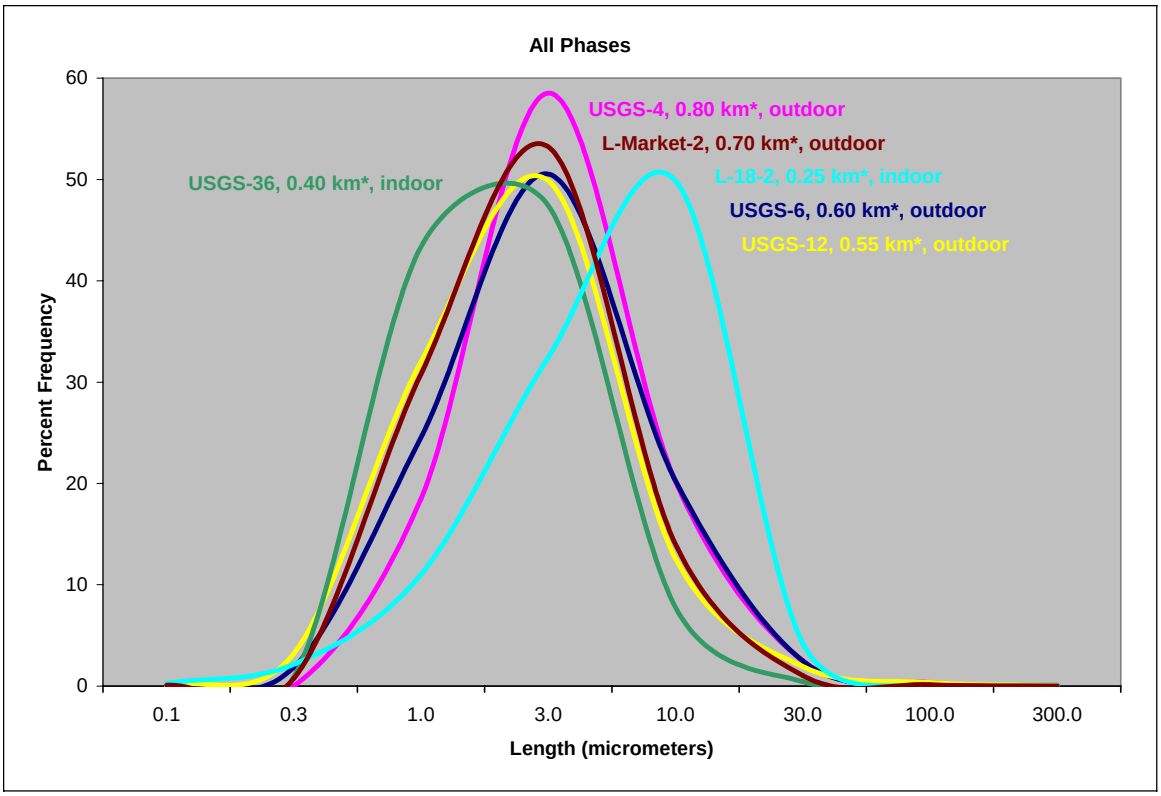

Figure 9. Particle size data for each sample presented as length vs. percentage frequency. *All distances are approximate kilometers from the center of WTC plaza.